

## Vacuum ultraviolet radiation of atomic nitrogen in pulsed self-sustained discharges of atmospheric pressure

© A.N. Panchenko, D.V. Beloplotov, V.A. Panarin, V.S. Skakun, D.A. Sorokin

Institute of High Current Electronics, Siberian Branch of the Russian Academy of Sciences, Tomsk, Russia

e-mail: alexei@loi.hcei.tsc.ru

Received April 16, 2025

Revised May 22, 2025

Accepted June 04, 2025

Parameters of vacuum ultraviolet (VUV) radiation of plasma jets and nanosecond diffuse discharges formed in gaps with a non-uniform electric field by high-voltage nanosecond pulses due to runaway electrons were studied. In nitrogen mixtures with helium or argon with a nitrogen content less than 10%, intense VUV radiation was detected on the atomic nitrogen lines at 149.3 and 174.3 nm. The compositions of gas mixtures for obtaining the maximum radiation power on these lines were determined. The average radiation power obtained was up to 6.8 mW/cm<sup>2</sup>. The volt-ampere and radiative characteristics of diffuse discharges in He(Ar)-N<sub>2</sub> mixtures were measured. An increase in the radiation intensity on the 149.3 and 174.3 nm lines after the cessation of the diffuse discharge current was detected.

**Keywords:** plasma jets, non-uniform electric field, diffuse plasma, nitrogen atoms, VUV radiation.

DOI: 10.61011/EOS.2025.07.61900.7802-25

### Introduction

Currently, research on plasma jets that form cold nonequilibrium plasma in mixtures of various atmospheric-pressure gases attracts great attention due to the wide application of such jets in different fields of science and technology [1,2]. This method of creating nonequilibrium plasma is distinguished by its simplicity and low cost of design. Most commonly, plasma jets based on various mixtures of atomic and molecular gases are used. For example, plasma jets formed in argon-nitrogen mixtures are effective sources of reactive species such as nitrogen atoms and metastable nitrogen molecules [3] and are widely used in medical applications for accelerating wound healing, sterilization of medical instruments, deactivation of viruses and bacteria, etc. [4–6]. Modeling of cold plasma impact parameters is also being conducted [7,8]. However, studies of the spectral composition of radiation from such plasma jets have often been limited to the visible and ultraviolet (UV) spectral ranges [1,9]. Several works have shown that the spectra of plasmas of various discharges in argon and helium mixtures with nitrogen or air include VUV lines of atomic nitrogen [10–12]. Detailed studies of the parameters of this emission were not performed.

The aim of this work is to investigate VUV radiation of atomic nitrogen in plasma jets and diffuse discharges formed in mixtures of nitrogen and air with helium and argon.

### Experimental Setup and Measurement Techniques

The experiments investigated the spectral characteristics of several types of self-sustaining discharges. To generate

plasma jets, a barrier discharge or a discharge between two thin metal electrodes with gas flow of nitrogen or air mixtures with inert gases through the discharge area was used. The designs of these devices are shown in Fig. 1. The barrier discharge was formed inside a quartz cavity, on the outer surface of which flat foil electrodes were placed (tube 1). The internal diameter of the tube at the plasma jet outlet was 4 mm. In another configuration, the discharge ignited inside a quartz tube with an internal diameter of 9 mm between two tungsten wires 0.3 mm in diameter, spaced 5 mm apart (tube 2). A high-voltage pulse generator with amplitudes up to 15 kV, pulse half-width of 100 ns, operating at frequencies up to 50 kHz was used to ignite the discharges.

In addition, emission spectra of a diffuse discharge between two needles with a gap of 4 mm between them were studied. Various generators of high-voltage nanosecond pulses were used to form the discharge [13]. The experimental setup for studying the parameters of diffuse discharge plasma is described in detail in [14]. The gap between the two needles was placed in a gas chamber and connected to a nanosecond high-voltage pulse generator with adjustable amplitude via a 3 m cable with impedance of 75 Ω. A series of direct and reflected pulses from the gap and generator with 30 ns intervals was applied to the gap. In some experiments, one of the needles was grounded through a 75 Ω load. In this case, only one or two voltage pulses were applied to the gap.

The chamber was attached to the input window made of LiF of a vacuum monochromator VM-502 (Acton Research Corp.) equipped with an EMI9781B photomultiplier (PMT), which recorded both the spectral distribution of the plasma discharge radiation energy in the range

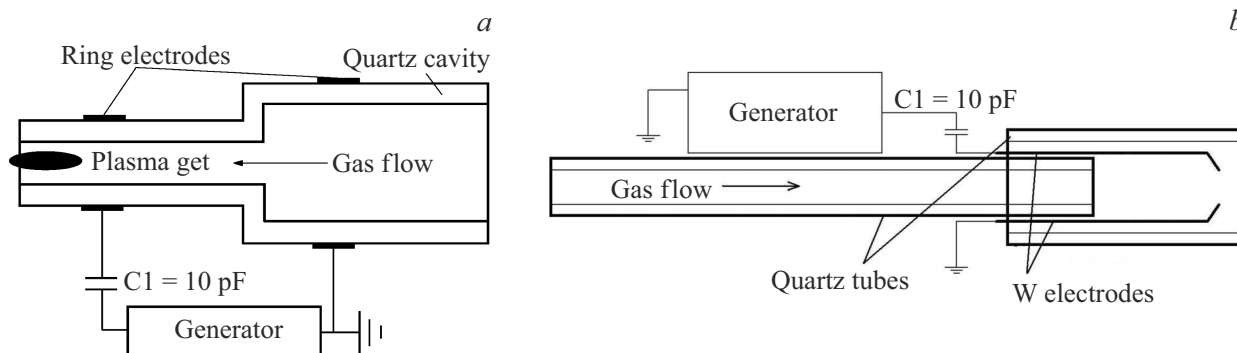


**Figure 1.** Schemes of plasma jet generation based on (a) barrier discharge, tube 1, and (b) spark discharge, tube 2.

100–545 nm, and the time evolution of radiation intensity at various wavelengths. The minimum rise time of the radiation pulse reliably recorded by the PMT is about  $\sim 3$  ns, the decay time about  $\sim 30$  ns. The monochromator was evacuated by an oil-free NORD-100 pump to a residual pressure of about  $10^{-6}$  Torr. A pulse generator BNC565 was used to trigger the high-voltage generator. The high-voltage generators used in the experiments had the following parameters: GIN 50-1 with an amplitude in the incident wave of up to +25 kV, duration at half-maximum  $t_{1/2} = 13$  ns, front  $t_f = 2$  ns; GIN 55-01 with an amplitude of up to –37 kV,  $t_{1/2} = 0.7$  ns,  $t_f = 0.7$  ns; GIN 100-1 with an amplitude of up to –25 kV,  $t_{1/2} = 4$  ns,  $t_f = 1$  ns; FPG with an amplitude of up to +13 kV,  $t_{1/2} = 1$  ns,  $t_f = 0.1$  ns.

For the registration of spectra, the plasma jets were directed at the entrance window of the gas chamber, made of  $\text{CaF}_2$  or  $\text{MgF}_2$  during this, the chamber was either evacuated to a residual pressure of  $10^{-3}$  Torr or filled with an inert gas. The power of VUV radiation was measured using a Hamamatsu C8026 Series meter with an H8025-126/146 sensor (sensitivity range at the 0.1 level from 140–185 nm, with maximum sensitivity at approximately 175 nm).

Additionally, the spectra and emission pulse shapes in the visible and UV ranges were recorded using an EPP2000C-25 spectrometer (StellarNet Inc.) with known spectral sensitivity and a vacuum coaxial photodiode FEC-22 with a time resolution of  $< 1$  ns. Voltage pulses at the input of the discharge chamber were recorded by a capacitive voltage divider. The waveforms of electrical signals were captured by Tektronix TDS-3054B digital oscilloscopes (500 MHz,  $5 \text{ Gs s}^{-1}$ ).

## Results of Experiments and Discussion

Figure 2 shows characteristic oscillograms of voltage on barrier discharge electrodes, generator circuit current, and a photo of the plasma jet. The electrode voltage rose over about 100 ns; after breakdown of the gap, oscillations of current and voltage in the pump circuit continued for

5–6  $\mu\text{s}$ . The discharge had an ellipsoidal shape, stretched along the gas flow.

In the initial experiments, a significant change in the plasma jet spectrum was observed depending on the distance from the quartz tube cut to the chamber entrance window (Fig. 3). At a distance of no more than 1–2 mm from the window, the emission spectrum showed a VUV continuum consisting of many lines attributed to transitions of the Lyman-Birge-Hopfield band ( $a^1\Pi_g - X^1\Sigma_g^+$ ) of molecular nitrogen [15]. This band usually appears in discharge or beam plasma radiation in nitrogen and air at gas pressures below  $10^{-4}$  Torr [16,17]. In the UV and visible regions, the most intense transitions were those of NO molecules, second positive and first negative systems  $\text{N}_2$ , with intensity maxima at 314, 337, 357, and 392 nm, as well as argon atomic transitions in the 410–550 nm range [9,18]. No argon second continuum emission with intensity maximum around 126 nm was observed.

Using a window made of  $\text{CaF}_2$  a calcium fluoride luminescence band in the 205–250 nm region was observed in the spectrum, apparently caused by VUV radiation from the plasma jet. The blue edge of this emission was shifted by about 20 nm, and the luminescence band was significantly narrower compared to the luminescence band of this material excited by a subnanosecond electron beam with electron energy  $> 50$  keV and current density up to  $j_b \approx 75 \text{ A/cm}^2$  [19]. The luminescence band of  $\text{CaF}_2$  itself should also be distinguished in the obtained spectrum. In subsequent experiments, a window made of  $\text{MgF}_2$  was used, which did not alter the discharge plasma emission spectrum.

When the tube cut was moved away from the  $\text{MgF}_2$  window, two VUV lines appeared in the discharge spectrum, whose intensity depending on the distance to the window could exceed the intensity of the second positive system nitrogen bands by 5–10 times! These lines corresponded to transitions  $3s^2P - 2p^2P^\circ$  and  $3s^2P - 2p^2D^\circ$  of atomic nitrogen at 174.3 and 149.3 nm respectively [20]. Obviously, the appearance of these lines is related to interactions of plasma components with nitrogen molecules as the jet passes through air.

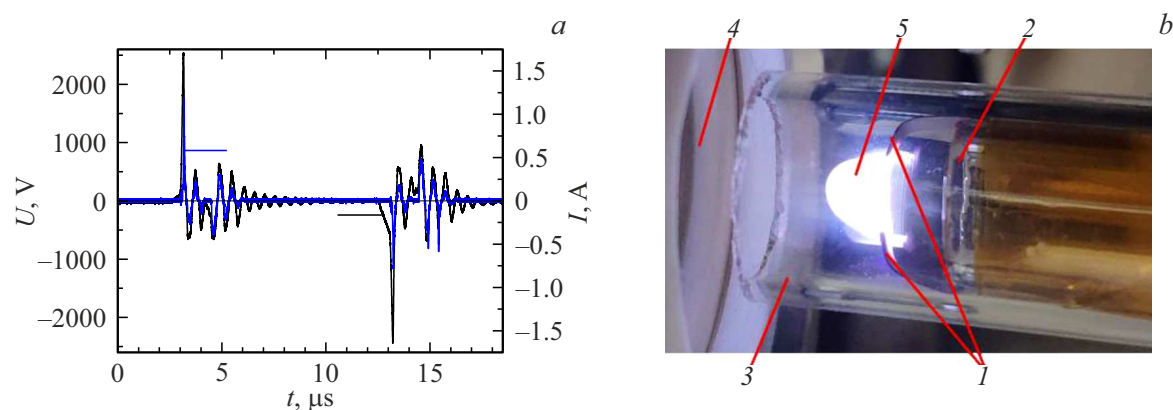


**Figure 2.** (a) Oscillograms of voltage pulses on the electrodes and current in the pump circuit, generator pulse amplitude 6 kV, argon flow 20 l/min, tube 1. (b) Appearance of the discharge in tube 2: 1 — tungsten electrodes, 2 — inner tube, 3 — outer tube  $\text{MgF}_2$  window, 5 — plasma jet.

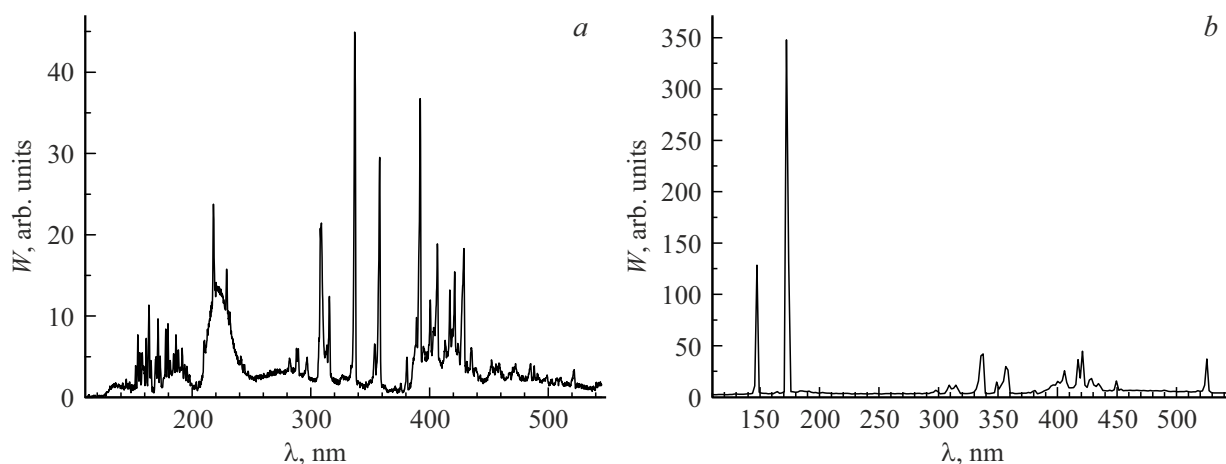


**Figure 3.** Radiation spectra of an argon plasma jet with the exit section of the tube positioned at 1 (a) and 7 mm (b) from the entrance window of the chamber. Tube 1, argon flow 20 l/min. Entrance window in the chamber from  $\text{CaF}_2$  (a) and  $\text{MgF}_2$  (b).

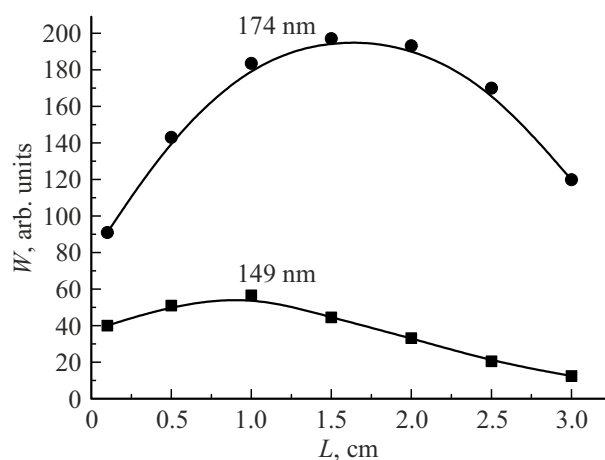


**Figure 4.** Intensities of atomic nitrogen lines from the argon jet discharge at various distances of tube cut from the  $\text{MgF}_2$  window. Tube 2, argon flow 10 l/min.

Figure 4 shows the intensity dependencies of atomic nitrogen lines from the discharge in a pure argon jet on the distance from the cut of tube 2 to the chamber window. The maximum radiation power was obtained when the tube end was 1–2 cm away; then the VUV intensity began to decrease due to absorption by oxygen contained in the air. VUV emission at the lines of 149 and 174 nm was observed even at the minimum distance of the tube cut from the chamber window, caused by air inflow into the discharge region through the gap between quartz tubes. A similar result was obtained in [10] when 0.1% air was added to an argon plasma jet. Increasing air inflow led to discharge instability; the gap might fail to break down for several generator pulses, reducing VUV line intensities. When the gap between tubes was sealed, VUV emission of atomic nitrogen at small tube-window distances was not detected. Therefore, subsequent studies focused on spectra of discharges ignited in flows of various inert gas-nitrogen

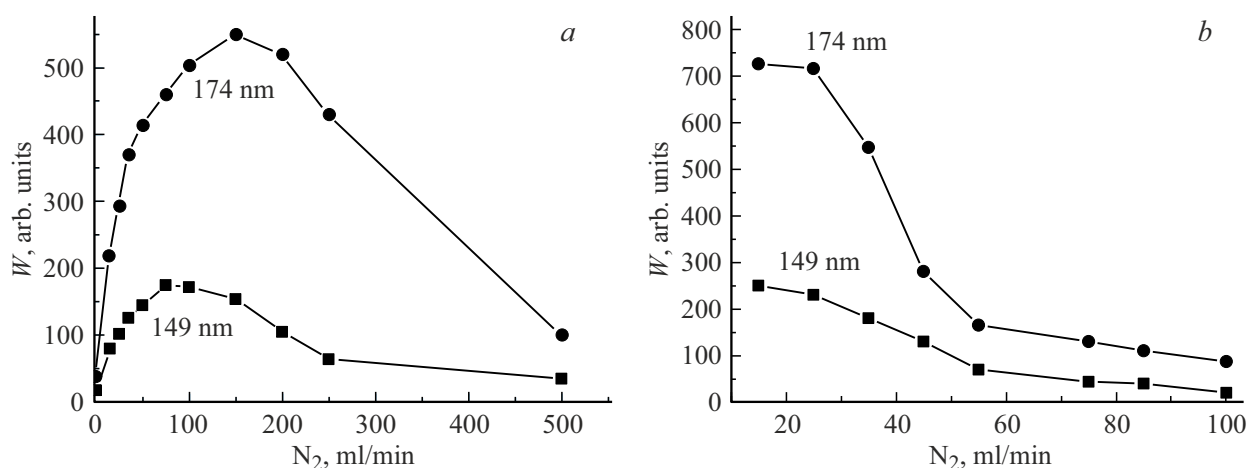


**Figure 5.** Dependencies of nitrogen VUV line emission intensities on nitrogen flow in the gas stream. Argon flow (a) and helium (b) 5 l/min. Tube 2. Nitrogen content in the mixture: 0–10% (a) and 0.2–2% (b).

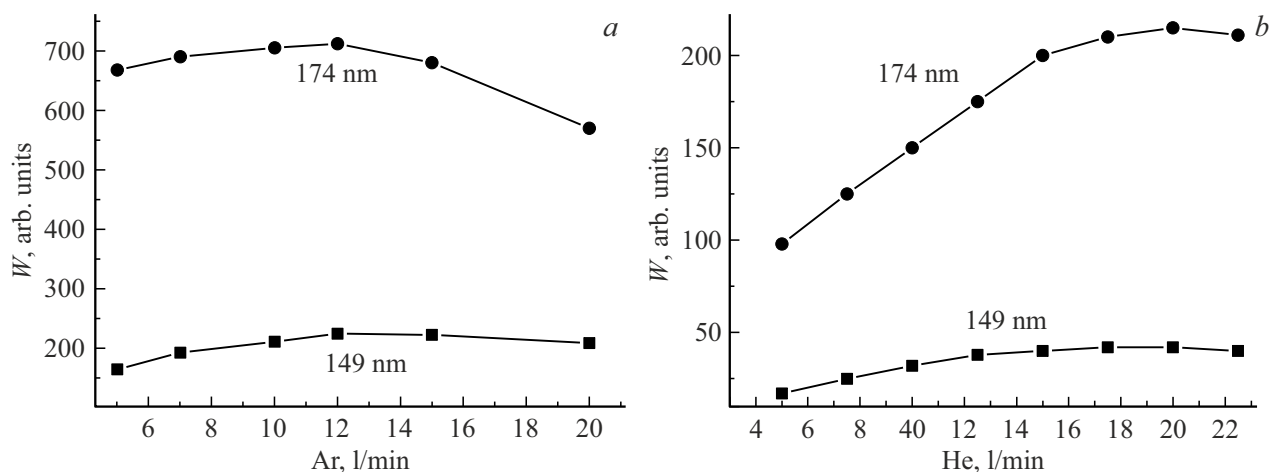


**Figure 6.** Dependencies of the nitrogen VUV line emission intensity on argon (a) and helium (b) flow rates in the gas stream. Nitrogen flow 0.1 l/min. Tube 2. Nitrogen content in the mixture: 2–0.5% (a) and 2–0.43% (b).

mixtures with controlled component flow ratios. Results are shown in Figs. 5 and 6.

Gas mixture compositions with argon and helium for maximum VUV emission power differed significantly. The intensity maximum for argon was reached at nitrogen flows of 0.1–0.15 l/min, while for helium the optimal nitrogen flow did not exceed 10–20 ml/min. Optimal argon and helium flows were 12 and 20 l/min, respectively. Adding air to argon or helium flows reduced nitrogen line intensity by 3–4 times already at 0.05 l/min air flow, and at 0.2 l/min air flow, VUV lines in the plasma jet spectrum were not detected.

Maximum VUV power on nitrogen lines in optimal gas mixtures increased with voltage pulse amplitude. For tube 1, it reached 2.8 mW/cm<sup>2</sup>; for tube 2, the emitted power increased approximately 2.5 times to 6.8 mW/cm<sup>2</sup>, comparable to xenon dimer barrier excilamp radiation power at 172 nm [21]. This VUV power in the plasma jet

remained almost unchanged when high-purity gases were replaced by technical grade gases with 99.99% purity, not requiring expensive inert gases or quartz tubes with high VUV transmission. Nitrogen line emission power could further increase with higher pulse voltage amplitude and repetition frequency, whereas xenon dimer lamp emission parameters in [21] are near their limits.

The relatively low pump pulse power in these discharge configurations did not allow temporal dependence measurements of emission power on atomic nitrogen lines. Therefore, diffuse discharge formed by powerful ns-pulse generators was used to measure emission pulses at 149 and 174 nm. Figure 7 shows volt-ampere and emission parameters of diffuse discharges in nitrogen-argon and nitrogen-helium mixtures.

From Fig. 7, the diffuse discharge forms upon the first generator pulse across the gap for both positive and negative polarities. Then energy is deposited into the discharge

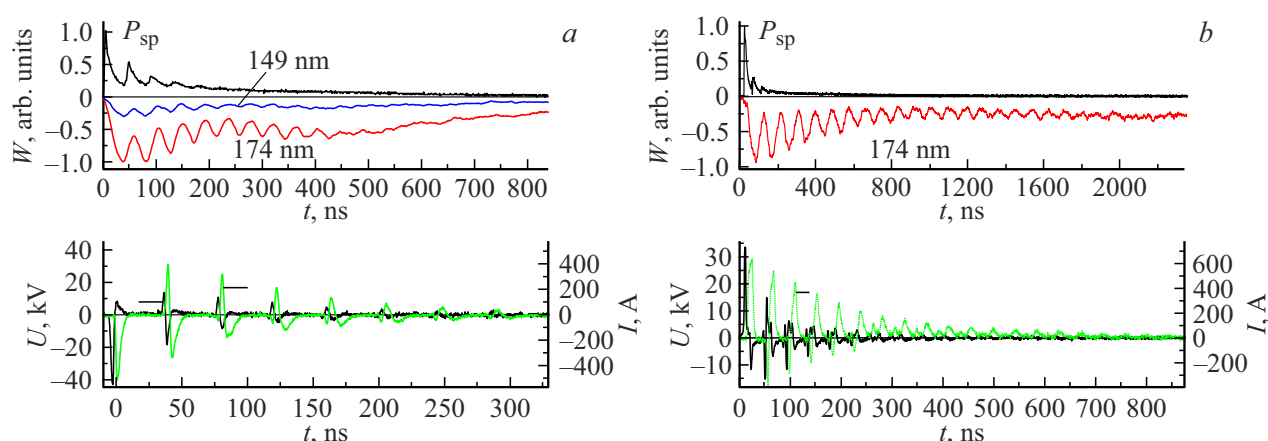


**Figure 7.** Oscillograms of diffuse discharge radiation pulses in the visible and UV regions ( $P_{sp}$ ) at wavelengths of 149 and 174 nm, as well as oscillograms of the signal from the capacitive divider ( $U$ ) and the discharge current ( $I$ ). The diffuse discharge is formed (a) — in the flow of the Ar:N<sub>2</sub> mixture with the speeds of 5 l/min:22 ml/min (the nitrogen content in the mixture is 0.44%), the generator GIN-100-5, 30 kV and (b) — in the He:N<sub>2</sub> mixture at the pressures of 2 atm:3 Torr (He:N<sub>2</sub>=99.8:0.2%), the generator GIN-50-1, 25 kV.

plasma by a train of reflected pulses over several hundred nanoseconds. After pumping ceases, a secondary increase in emission intensity at 149 and 174 nm is observed. This indicates that a relaxation plasma energy transfer channel exists to the upper level of these VUV transitions. Emission spectra under these conditions were similar to those shown in Fig. 3, *b*. The intensity of the VUV lines significantly exceeded the intensity of emission from the second positive system of nitrogen, which is unusual for diffuse discharges in mixtures with N<sub>2</sub> [12], and noticeably increased with the rise in voltage pulse amplitudes from the generators.

Similar discharge parameter behavior is observed when it is formed by a single pulse (Fig. 8, *a*). Here, an increase in VUV emission intensity after the excitation pulse ends is also visible. However, under these experimental conditions, the intensity of atomic nitrogen emission decreases by more than an order of magnitude compared to emission from plasma jets and diffuse discharges excited by a pulse series (fig. 8, *b*). This can be explained by the integral photographs of the diffuse discharge shown in Fig. 9. When a single 1 ns pulse is applied to the gap, the diffuse discharge forms as a blue streamer about 2 mm wide, similar to the results provided in [22,23]. Increasing the pump pulse duration causes the diffuse discharge to transition to a channel stage, reducing its width by approximately three times. A pink halo surrounds the channel, caused by emission of the first positive system of nitrogen from the expanding channel, continuing for several tens of microseconds after the discharge current ends. These data indicate that to achieve efficient emission on nitrogen VUV lines, it is necessary to increase the discharge current density, which enhances electron-impact dissociation of nitrogen molecules and increases atomic nitrogen concentration in the discharge plasma. The increase in VUV emission power in the wire-to-wire discharge can also be attributed to higher current density in tube 2 compared to tube 1.

The peaks in spontaneous emission pulses in UV and visible spectral regions in Figs. 7 and 8 mimic the peaks of excitation pulses. Pulses at 147 and 174 nm lines began several nanoseconds after gap breakdown, reaching maximum intensity within about 30–40 ns, after which VUV emission intensities oscillated with a period close to the period of discharge current pulses. Peaks of emission and current pulses did not coincide due to front delays in photomultiplier tube optical signals from the monochromator. Analysis of the diffuse discharge emission spectrum formed by a single pulse from the GIN 55-01 generator showed that during the first nanoseconds after gap breakdown, emission pulses from nitrogen ion at 391 nm and nitrogen molecule at 337 nm appear. These pulses peak at 10 and 15 ns, respectively, and cease after  $\sim 50$  ns. VUV emission pulses are delayed by a few nanoseconds with a rising front of  $\sim 35$  ns followed by a smooth intensity decay. It is known that the upper level of the 337 nm transition is populated by direct electron impact [24]. The difference between UV and VUV pulses indicates that direct electron impact is not the main channel for populating the  $^2P$  atomic nitrogen level.

Additional experiments and modeling calculations are required to determine the population channels of the upper levels of atomic nitrogen VUV transitions. For example, in argon mixtures, possible population channels of the  $^2P$  atomic nitrogen level may include collisional energy transfer from long-lived metastable argon levels Ar\* cascade transitions from a long-lived ( $> 100$  ns) atomic nitrogen level  $^2S$  with excitation energy of 11.6 eV, which can be effectively populated in collisions with argon metastables Ar\* ( $^3P_0$ ) (11.72 eV), accompanied by photon emission at 1345.6 nm, or relaxation of level  $^2S$  to  $^2P$  by collisions with Ar atoms [25–27].

In the case of helium mixtures, this mechanism for populating the  $^2P$  level will not operate. Experiments



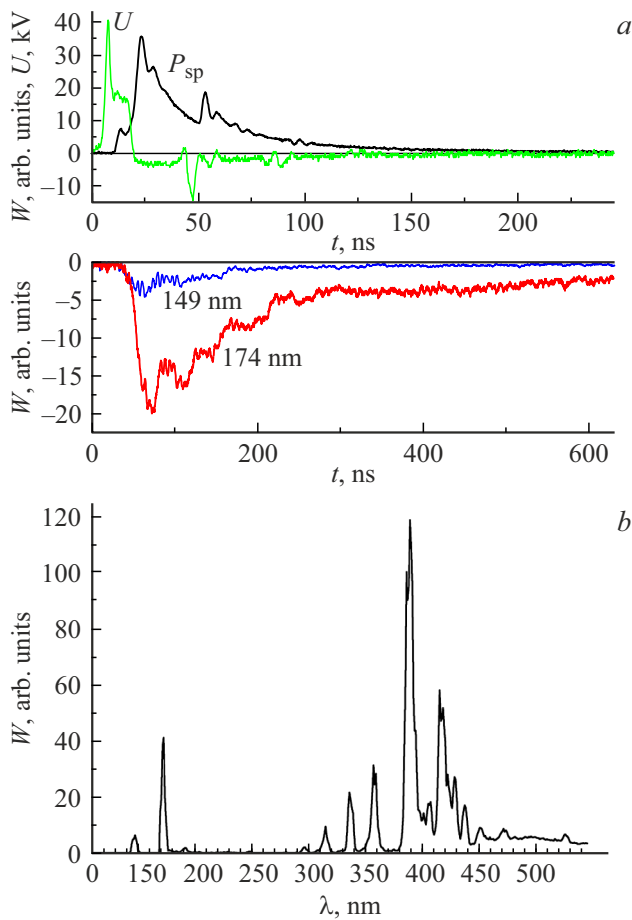
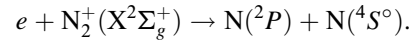


**Figure 8.** Oscillograms of diffuse discharge radiation pulses in the visible and UV regions ( $P_{sp}$ ) and on the 149 and 174 nm lines, as well as oscillograms of the signal from the capacitive divider ( $U$ ), (b) discharge spectrum. A diffuse discharge is formed in a mixture of He:N<sub>2</sub> at pressures of 2 atm:3 Torr (He:N<sub>2</sub>=99.8:0.2%). Generator GIN-50-1, 25 kV, load connected 75 Ω.

conducted in [3,12] showed that during the voltage decay stage at high electric field strengths across the gap, emission from the second positive system of nitrogen first appears, with an intensity noticeably higher than that of the VUV lines. After the voltage decay and current increase in the gap, leading to discharge contraction, the VUV lines appear with a delay of several nanoseconds, and their intensity significantly exceeds that of the 2<sup>+</sup>-system. This indicates that in the initial discharge stage, direct ionization processes of nitrogen molecules dominate. These works suggest that the main mechanism for forming excited atomic nitrogen may be a two-step process. During discharge formation, nitrogen molecules dissociate via direct electron impact; then, under high current density conditions, nitrogen atoms in the N(<sup>2</sup>P) state arise from collisions between electrons and nitrogen atoms in the ground state N(<sup>2</sup>D°) and excited state N(<sup>2</sup>P°) [3,12]. As noted above, in our experiments, VUV line intensity also increased with higher discharge current density. Other kinetic processes in gas-

discharge plasma leading to nitrogen molecule dissociation are discussed in detail in [28].

In experiments [29] VUV lines appeared with a delay after streamer closure of the gap. The population of the upper VUV transition levels was associated with dissociative recombination of the molecular nitrogen ion in the ground state via the following process:



After the discharge current ceases, the main channel populating the N(2P) level may be collisions of vibrationally excited nitrogen molecules in the metastable state  $_2(A^3\Sigma_u^+, \nu)$  with nitrogen atoms in the states N(<sup>2</sup>P°) and <sup>2</sup>D° [30], which are also metastable with lifetimes of 11 and 49000 s, respectively [31].

It should be noted that [32] reports the possibility of achieving amplification on atomic nitrogen lines. To verify the possibility of lasing at 149.3 and 174.3 nm lines, measurements of VUV emission from an extended diffuse discharge using an experimental setup with long blade electrodes are planned [14].

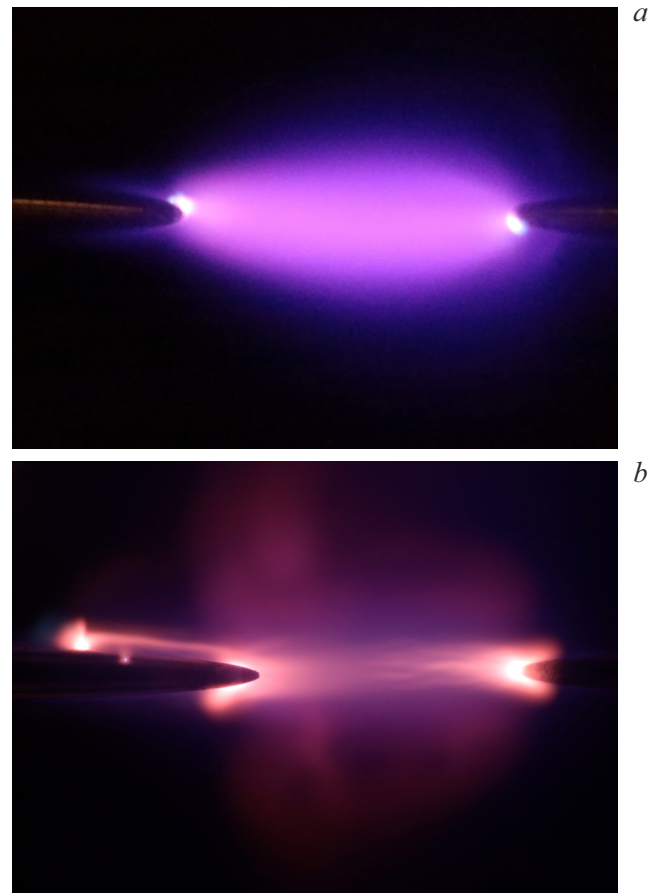


**Figure 9.** Integral photographs of diffuse discharge in a mixture of He:N<sub>2</sub> at pressures of 1 atm:3 Torr (He:N<sub>2</sub>=99.6:0.4%). A single pulse (a) or a pulse series (b) is applied to the gap. FPG-10 (a) and GIN 50-1 (b) generators.

## Conclusion

It has been shown that plasma jets and diffuse discharges formed in gaps with non-uniform electric fields by nanosecond high-voltage pulses, due to runaway electrons in argon, helium, and nitrogen mixtures, are sources of intense VUV emission of atomic nitrogen at wavelengths of 149 and 174 nm. Optimization of mixture compositions and plasma jet generation conditions was performed to achieve maximum emission power on atomic nitrogen lines. An average emitted power of up to 6.8 mW/cm<sup>2</sup> was obtained.

Volt-ampere and emission characteristics of diffuse discharges in He(Ar)–N<sub>2</sub> mixtures were measured. It was found that emission intensity at wavelengths 149 and 174 nm increases after the diffuse discharge current ceases. The possibility of stimulated emission on atomic nitrogen lines was proposed.

It was demonstrated that to increase emission intensity on nitrogen atom VUV lines, it is necessary to increase the discharge current density.

## Funding

This study was carried out under the state assignment of the Institute of High Current Electronics of the Siberian Branch of the Russian Academy of Sciences (project No. FWRM-2021-0014).

## Conflict of interest

The authors declare that they have no conflict of interest.

## References

- [1] A. Barkhordari, A. Ganjovi, I. Mirzaei, A. Falahat, M.N. Rostami Ravari. *J. Theor. Appl. Phys.*, **11** (4), 301 (2018). DOI: 10.1007/s40094-017-0271-y
- [2] Tao Shao, Ruixue Wang, Cheng Zhang, Ping Yan. *High Voltage*, **3** (1), 14 (2018). DOI: 10.1049/hve.2016.0014
- [3] V. Ferrer, J.-P. Gardou, F. Marchal, A. Ricard, J.-P. Sarrette. *Eur. Phys. J. D*, **76** (10), 191 (2022). DOI: 10.1140/epjd/s10053-022-00512-5
- [4] I. Schweigert, D. Zakrevsky, P. Gugin, E. Yelak, E. Golubitskaya, O. Troitskaya, O. Koval. *Appl. Sci.*, **9** (21), 4528 (2019). DOI: 10.3390/app9214528
- [5] Susumu Suzuki, Kenji Teranishi, Haruo Itoh. *Electric. Engineer. Japan*, **217** (1), e23457 (2024). DOI: 10.1002/eej.23457
- [6] R. Kawakami, Y. Yoshitani, K. Mitani, M. Niibe, Y. Nakano, C. Azuma, T. Mukai. *Appl. Surf. Sci.*, **509**, 144910 (2020). DOI: <https://doi.org/10.1016/j.apsusc.2019.144910>
- [7] N.Y. Babaeva, G.V. Naidis, V.A. Panov, R. Wang, Y. Zhao, T. Shao. *Phys. Plasmas*, **25** (6), 063507 (2018). DOI: 10.1063/1.5024778
- [8] P. Viegas, E. Slikboer, Z. Bonaventura, O. Guaitella, A. Sobota, A. Bourdon. *Plasma Sourc. Sci. Technol.*, **31** (5), 053001 (2022). DOI: 10.1088/1361-6595/ac61a9
- [9] M.C. García, M. Varo, P. Martínez. *Plasma Chem. Plasma Process.*, **30** (2), 241 (2010). DOI: 10.1007/s11090-010-9215-x
- [10] R. Brandenburg, H. Lange, T. von Woedtke, M. Stieber, E. Kindel, J. Ehlbeck, K.-D. Weltmann. *IEEE Trans. Plasma Sci.*, **37** (6), 877 (2009). DOI: 10.1109/TPS.2009.2019657
- [11] Y. Kashiwagi, H. Ito, K. Noguchi, K. Teranishi, S. Suzuki, H. Itoh. *IEEJ Trans. Fund. Mater.*, **127** (9), 537 (2007). DOI: 10.1541/ieejfms.127.537
- [12] A. Fierro, G. Laity, A. Neuber. *J. Phys. D*, **45** (45), 495202 (2012). DOI: 10.1088/0022-3727/45/49/495202
- [13] V.M. Efanov, M.V. Efanov, A.V. Komashko, A.V. Kirilenko, P.M. Yarin, S.V. Zazoulin. in *2010 Ultra-Wideband, Short Pulse Electromagnetics 9*, part 5, p. 301–306 (Springer-Verlag, N.Y., 2010). DOI: 10.1007/978-0-387-77845-7
- [14] A.N. Panchenko, V.F. Tarasenko, V.V. Kozhevnikov. *Appl. Phys. B*, **129** (11), 178 (2023). DOI: 10.1007/s00340-023-08125-5
- [15] A. Lofthus, P.H. Krupenie. *J. Phys. Chem. Ref. Data*, **6** (1), 113 (1977). DOI: <https://doi.org/10.1063/1.555546>
- [16] U. Fantz, S. Briefi, D. Rauner, D. Wunderlich. *Plasma Sourc. Sci. Technol.*, **25** (4), 045006 (2016). DOI: 10.1088/0963-0252/25/4/045006
- [17] J.M. Ajello, J.S. Evans, V. Veibell, Ch.P. Malone, G.M. Holsclaw, A.C. Hoskins, R.A. Lee, W.E. McClintock, S. Aryal, R.W. Eastes, N. Schneider. *J. Geophys. Res.: Space Physics*, **125** (3), e2019JA027546 (2020). DOI: 10.1029/2019JA027546
- [18] S. Sintsov, K. Tabata, D. Mansfeld, A. Vodopyanov, Ki. Komurasaki. *J. Phys. D*, **53** (30), 305203 (2020). DOI: 10.1088/1361-6463/ab8999
- [19] D.A. Sorokin, A.G. Burachenko, D.V. Beloplotov, V.F. Tarasenko, E.Kh. Baksht, E.I. Lipatov, M.I. Lomaev. *J. Appl. Phys.*, **122** (15), 154902 (2017). DOI: 10.1063/1.4996965
- [20] D.A. Dahlberg, D.K. Anderson, I. E. Dayton. *Phys. Rev.*, **64** (1), 20 (1967). DOI: 10.1103/PhysRev.164.20
- [21] M.I. Lomaev, V.S. Skakun, V.F. Tarasenko, D.V. Shitts. *J. Opt. Technol.*, **79** (8), 498 (2012). DOI: 10.1364/JOT.79.000498
- [22] D.V. Beloplotov, V.F. Tarasenko, D.A. Sorokin, M.I. Lomaev. *JETP Lett.*, **106** (10), 653 (2017). DOI: 10.1134/S0021364017220064
- [23] N.Yu. Babaeva, G.V. Naidis, D.V. Tereshonok, V.F. Tarasenko, D.V. Beloplotov, D.A. Sorokin. *J. Phys. D*, **56** (3), 035205 (2023). DOI: 10.1088/1361-6463/aca776
- [24] A.W. Ali, A.C. Kolb, A.D. Anderson. *Appl. Opt.*, **6** (12), 2115 (1967). DOI: 10.1364/AO.6.002115
- [25] N. Masoud, K. Martus, K. Becker. *J. Phys. D*, **38** (11), 1674 (2005). DOI: [iopscience.iop.org/0022-3727/38/11/006](https://doi.org/10.1088/0022-3727/38/11/006)
- [26] C. Foissac, J. Krištof, A. Annušová, V. Martišovič, P. Veis, P. Supiot. *Plasma Sourc. Sci. Technol.*, **19** (5), 055006 (2010). DOI: 10.1088/0963-0252/19/5/055006
- [27] Hironobu Umemoto, Naoki Terada, Kunikazu Tanaka, Shigeki Oguro. *Phys. Chem. Chem. Phys.*, **2** (15), 3425 (2000). DOI: 10.1039/B003280H
- [28] A.V. Volynets, D.V. Lopaev, T.V. Rakhimova, A.A. Chukalovsky, Yu.A. Mankelevich, N.A. Popov, A.I. Zotovich, A.T. Rakhimov. *J. Phys. D*, **51** (36), 364002 (2018). DOI: 10.1088/1361-6463/aad1ca
- [29] N. Sewraj, N. Merbahi, J.P. Gardou, P. Rodriguez Akerreta, F. Marchal. *J. Phys. D*, **44** (14), 145201 (2011). DOI: 10.1088/0022-3727/44/14/145201

- [30] A. Rahman, A.P. Yalin, V. Surla, O. Stan, K. Hoshimiya, Z. Yu, E. Littlefield, G.J. Collins. Plasma Sourc. Sci. Technol., **13** (3), 537 (2004). DOI: 10.1088/0963-0252/13/3/021
- [31] A. Owens, T. He, M. Hanicinec, C. Hill, S. Mohr, J. Tennyson. Plasma Sourc. Sci. Technol., **32** (8), 085015 (2023). DOI: 10.1088/1361-6595/aceeb0
- [32] G.N. Gerasimov, E. Krylov, D.I. Stasel'ko, I.V. Alekseev. J. Opt. Technol., **79** (8), 462 (2012). DOI: 10.1364/jot.79.000462 10.1364/jot.79.000462

*Translated by J.Savelyeva*